

# Finger Movements Are Mainly Represented by a Linear Transformation of Energy in Band-Specific ECoG Signals

Ali Marjaninejad, *Member, IEEE*, Babak Taherian, *Member, IEEE*  
and Francisco J. Valero-Cuevas, *Senior Member, IEEE*

**Abstract**— Electrocorticogram (ECoG) recordings are very attractive for Brain Machine Interface (BMI) applications due to their balance between good signal to noise ratio and minimal invasiveness. The design of ECoG signal decoders is an open research area to date which requires a better understanding of the nature of these signals and how information is encoded in them. In this study, a linear and a non-linear method, Linear Regression Model (LRM) and Artificial Neural Network (ANN) respectively, were used to decode finger movements from energy in band-specific ECoG signals. It is shown that the ANN only slightly outperformed the LRM, which suggests that finger movements are mainly represented by a linear transformation of energy in band-specific ECoG signals. In addition, comparing our results to similar Electroencephalogram (EEG) studies illustrated that the spatio-temporal summation of multiple neural signals is itself linearly correlated with movement, and is not an artifact introduced by the scalp or cranium. Furthermore, a new algorithm was employed to reduce the number of spectral features of the input signals required for either of the decoding methods.

## I. INTRODUCTION

The use of biological signals has a broad spectrum including online patient monitoring, drug delivery control [1], reduction of limitations for disabled patients [2], [3], medical monitoring and decision making [4], [5], or even providing entertainment [6]. Cerebral activity produces biological signals which can provide enough information to interact with the surrounding, even in the absence of peripheral nerves and muscles [6]. The hardware and software enabling this interaction is called brain machine interface (BMI), also referred to as brain computer interface (BCI) [6]. BMI is considered to have the potential for restoring locomotor ability in patients with movement disorders as a result of brain injury or deterioration. The main purpose of medical BMIs is to decode or replicate the neural signals responsible for proper functioning of the damaged or paralyzed body parts [7]. One of the most important tasks in upper limb prosthetics is finger control and having a better understanding of how the nervous system controls finger movements can help in selecting best strategy to control prosthetics and increase their performance [8], [9].

A. Marjaninejad, B. Taherian and F. J. Valero-Cuevas are with the Department of Biomedical Engineering, University of Southern California, Los Angeles, CA 90089 USA (e-mail: marjanin@usc.edu, btaheria@usc.edu, valero@usc.edu).

F. J. Valero-Cuevas is also with the Division of Bio-kinesiology and Physical Therapy, University of Southern California, Los Angeles, CA 90089 USA.

Currently used methods for recording the electrical activity of the brain include the electroencephalogram (EEG), Magnetoencephalography (MEG), electrocorticogram (ECoG), local field potential (LFP), and single-unit activity/multi-unit activity (SUA/MUA) [3], [6], [10]–[12]. In ECoG recordings, since the electrodes are placed under the scalp, spatial resolution and signal to noise ratio are higher than MEG or EEG recordings. Also, unlike MEG, ECoG does not need bulky hardware, and thus is more portable and better suited for long term use. Moreover, compared to intra-cortical recordings like LFP, SUA/MUA, ECoG is less invasive [13], [14].

Here, we have used two of the most common ECoG (and EEG) decoding algorithms, Linear Regression Model (LRM) [13] and Artificial Neural Network (ANN) [11], for detection and estimation of finger movements from the ECoG signals in human subjects. LRM assumes there are linear relationships between the input and output sets and provides the coefficients for the linear equations which map inputs to outputs. ANN, on the other hand, is a machine learning technique which is not limited to linear relationships and can model non-linearity and map inputs to the output space. Although the brain does not work in a linear fashion, high dimensionality and noise in cerebral recordings can make it very challenging for the non-linear systems to decode these signals [15].

The goal of this paper is not only finding the best approach to decode ECoG signals, but also providing information on the nature of the finger movements represented at the ECoG level. The latter will also greatly contribute to the design of more efficient BMI devices which are controlled by ECoG signals. In addition, by comparing and contrasting these findings with similar findings from EEG studies [15], we can determine a better understanding about the effects of the skull on the cerebral signals. We have also introduced a simple method to selectively reduce the number of input features in order to decrease the computational cost of the decoding. Finally, we have designed a finger movement detector to be able to compare results in both estimation (continuous finger movement estimation) and decision making (deciding if the finger is moving or not) paradigms.

## II. METHODS

### A. Sub-band Decomposition

Different brain activities can increase the activity level of the ECoG signals in different frequency bands unequally [13]. Therefore, an FIR filter bank was used to decompose the recorded signals into three different sets of band-specific ECoG signals. These bands include slow potential sub band

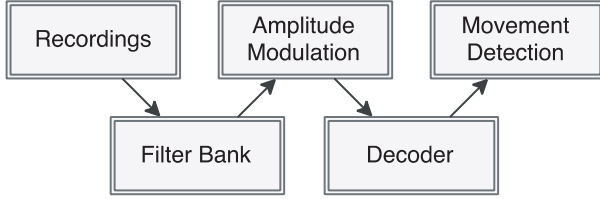


Fig. 1. The schematic representation of the system

(1-60 Hz), gamma band (60-100 Hz), and fast gamma band (100-200 Hz). The schematic representation of this filter bank and its connection to the other parts of the system is shown on Fig. 1. Also, the frequency responses of the filters are illustrated on Fig. 2. A short sample of the ECoG signal and its sub-band decomposition as functions of time are shown on Fig. 3. In addition, the corresponding thumb movements for the same signals are illustrated on Fig. 4.

### B. Feature Extraction

Similar to [13], inspired by the spike rate coding approach [16], a band specific amplitude modulation was used as a descriptor for ECoG signal decoding. This amplitude modulation is defined as the sum of the square voltage values of the band-specific ECoG signals  $v$  in a time window  $\Delta t(t_{n+1} - t_n)$ . The amplitude  $x$ , for each time point  $t_n$  is defined as follows:

$$x(t_n) = \sum_{t=0}^{\Delta t} v^2(t_n + t) \quad (1)$$

$\Delta t$  was set to 40 ms so that the resulting band specific AM features have the same sampling rate as that of the data-glove position measurements. The 400,000 samples were thus reduced to 10,000 after applying the amplitude modulation mentioned above. Please note that each  $x(t_n)$  represents energy of the signal in the corresponding time bin. A sample representation of these features is shown on the Fig. 5.

### C. Memory Features

As discussed earlier, there are three band specific ECoG signals recorded from each electrode (total of 62 electrodes) including slow potential sub band, gamma band and fast gamma band (total of 3 bands). It is known that finger movement depends on the present state of brain activity as well as previous states. In this specific experiment, based on previous work [13], the last 25 states used as the decoder input resulted in a total of 4650 ( $62 \times 3 \times 25$ ) features for each instant in time.

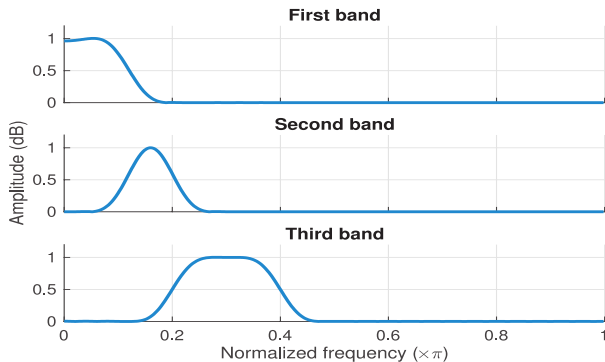


Fig. 2. Frequency response of different bands of the filter bank.

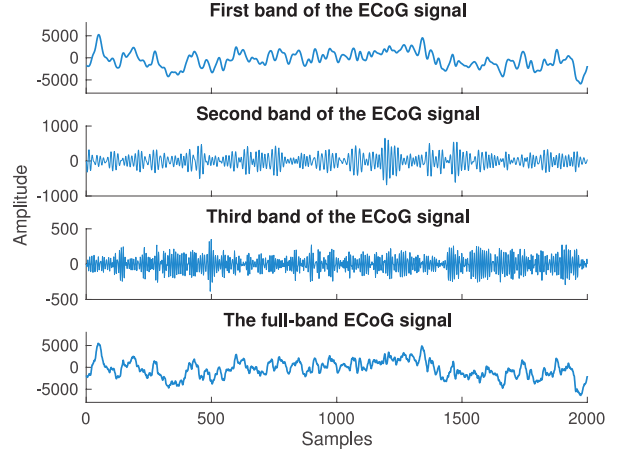


Fig. 3. A sample of sub-band decomposition of the ECoG signal. First three plots (from up to the down) show the low, middle, and high frequency bands respectively and the one on the bottom shows the original ECoG signal.

### D. Decoder models

As discussed earlier, in this paper, we have used two of the most common decoders in the field. LDR, as the linear decoder, and ANN as the non-linear decoder. The details of each method are described in this section.

#### 1) Linear Regression Model

To model the relation between brain activity and hand movements, we used a linear regression model. Equations describing this model are as follows [13]:

$$d(t_n) = W^T \vec{x}(t_n) \quad (2)$$

where  $d$  is finger position as measured by the data-glove and  $\vec{x}(t_n)$  is the short-term memory AM feature vector described as:

$$\vec{x}(t_n) = [\vec{x}(t_n) \vec{x}(t_{n-1}) \vec{x}(t_{n-2}) \dots \vec{x}(t_{n-k})]^T \quad (3)$$

where  $k$  is the number of the previous states stored. The coefficients matrix of the model,  $W$ , is trained with the Wiener solution:

$$W = (\vec{x}^T \vec{x})^{-1} (\vec{x}^T d) \quad (4)$$

Since the inverse matrix operator in MATLAB software has a high computational weight, alternatively, the pseudo-inverse operator was used.

#### 2) Artificial Neural Networks (ANN)

Neural networks are one of the machine learning algorithms which has attracted an increasing amount of attention due to its high performance in a variety of applications [6], [15]. These networks are inspired by how the brain works and are able to model complex systems by mapping inputs into output space. ANNs also enables us to

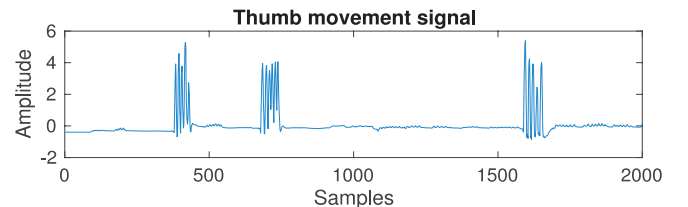


Fig. 4. A sample finger (Thumb) movement signal.

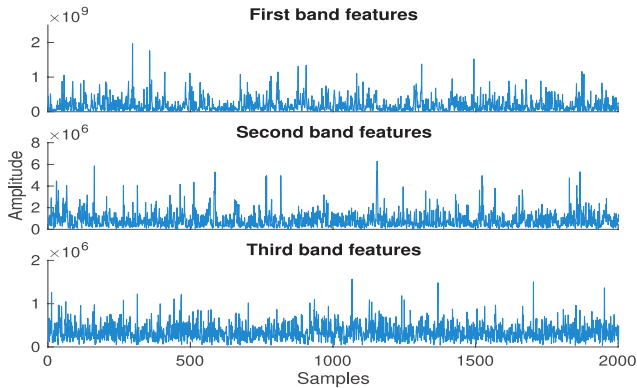


Fig. 5. A sample representation of input features.

produce nonlinear decision boundaries [6].

Since ANN can model non-linear relationships between input and output data, comparing its results with the LRM will provide us with a better understanding about the type of relationship between finger movements and ECoG signals. Here we used a feed-forward Multi-Layer Perceptron (MLP) ANN with one hidden layer (6 neurons in the hidden layer), trained with the Back Propagation (BP) algorithm. The TANSIG function was used as the transfer function for hidden layers while the PURELINE function was used for the final layer. The schematic structure of the ANN used in this study is illustrated in Fig. 6. We also increased the number of hidden layers (and their neurons) to see how increasing the number of hidden layers or hidden layer neurons affects the performance of the system.

#### E. Reducing the size of the feature vector

It is clear that not all the electrodes/bands have the same amount of hand movement information. Therefore, it is computationally optimal to find the features which have the most information and subsequently reduce the size of the feature vector by using the most relevant features pertaining to the task.

In previous studies, sub-optimal trial and error methods were being used [13]. In this study, we used a fast, yet accurate, algorithm to find the most important features. We calculated the LRM weights for a short period of time (2000 samples) and then sorted them based on the amplitude of their weights which corresponds to the correlation of the input signals and the output finger movements. Finally, we selected the first 200 features. We've also tested both algorithms, randomly selecting 200 features, in order to verify that decoding using features selected by our selection method always outperforms decoding using any other set of features with the same size.

#### F. Post-filtering

In this stage, to identify the time periods in which we had finger movements, we applied a zero-phase moving average (low pass FIR) filter to smoothen the output signal. The smoothened output will avoid frequent on-and-offs during finger movements for the threshold comparator described in the next section.

#### G. Finger movement detector

In the previous section, the maximum amplitude of the train data, when there was no finger movement, was

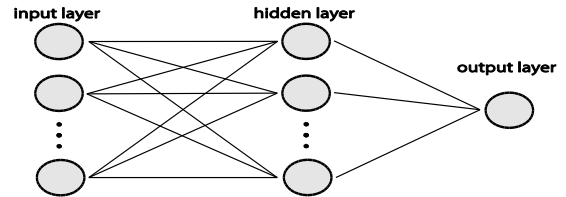


Fig. 6. The schematic structure of the MLP ANN used in this study.

multiplied by an empirically chosen coefficient (in this study, this coefficient was set equal to 1.25) and set as the threshold value to determine whether there was any movement or not. The schematic representation of the connection between all the different parts of the system is illustrated on the Fig. 1.

### III. RESULTS

We have used the dataset described in [17] to demonstrate our results. The proposed algorithm for reducing the size of the feature vector leads to a 60-fold increase in the computational speed compare to the LRM approach without decreasing the size of the feature vector. Training a three-layer feed-forward MLP with about 50 neurons without decreasing the feature size of the dataset used in this study is not computationally feasible or at least reasonable using commercially available computers. Moreover, none of the two decoding methods performed better using randomly selected features, showing that our feature selection algorithm does not compromise performance.

The implemented LRM using the described feature selection method could achieve promising precision rates (by means of correlation) compared to previous studies. In addition, the ANN model outperformed the LRM only by a slight difference, emphasizing that although the functions which map the energy in the band-specific ECoG signals to finger movements are non-linear, they can be modeled linearly with acceptable error compared to non-linear approaches. Also, increasing the number of hidden layers/neurons in the ANN decreased its performance. This shows that the non-linear relationship between the input and output space is not considerable and the ANN will suffer from overfitting when increasing the number of hidden layers. The correlation values for real finger movements and estimation finger movements of all five fingers for the two models used in this paper are provided in Table I. These results were achieved by having 70% of the data as train data and the other 30% as test data. Please note that weights in both algorithms were calculated separately for each finger.

After applying the post filter and incorporating the threshold comparator, the system could accurately report all finger movement spans using only ECoG signals as the input. The movement decoding, smoothed output, and the movement interval indicators for the LRM method, are illustrated on the Fig. 7. These results are for the test dataset and the system was not exposed to this data during the training phase.

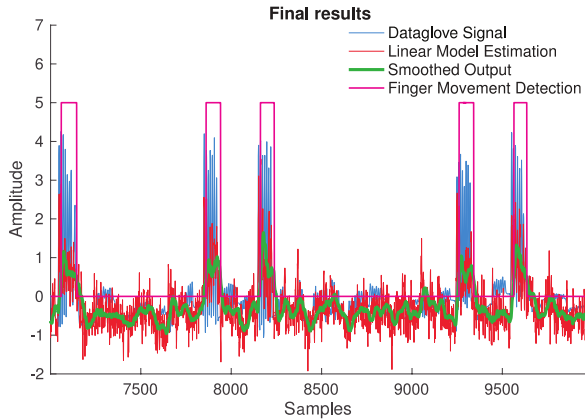


Fig. 7. Finger movement, finger movement estimation, smoothed estimation and the movement interval indicator signals.

#### IV. DISCUSSION

Both the LRM and ANN methods were able to detect and track finger movements with acceptable performance. The ANN outperformed the LRM only by a slight difference. It suggests that finger movement information is mainly a linear function of the energy in band-specific ECoG signals. It was also observed that the precision of the ANN method decreased when the number layers or the number of hidden layer neurons increased which in turn suggests that increasing the complexity of the model to catch more non-linearity in the input output mapping will lead to overfitting. This shows, once again, that the relationship between finger movements and energy in band-specific ECoG signals, consists mainly of linear nature.

We believe spatial filtering of neurons under a single electrode and recording noise will cancel out or distort non-linear aspects of the data and make it very challenging for non-linear techniques to outperform linear ones.

The feature selection algorithm used in this study selects features based on their performance in a short time run using the LRM. One might argue that this approach only focuses on features with a linear relationship to the output and leaves the features with a non-linear relationship out; therefore, it will bias our observations on the input-output relationship being mainly linear. However, this is not the case. First, these features are the ones which were the most active and had maximum correlation with the output. Although this is a linear correlation, it does not stop the ANN from finding any non-linear relationships within the selected features and the output space. Secondly, none of the decoding methods used performed better when using randomly selected features, which again suggests that hand movements are mainly represented by a linear transform of the energy in band-specific ECoG signals.

Finally, the results in this study are consistent with [15] where it is shown that non-linear decoding methods perform only slightly better than linear ones for EEG signals. This advocates that the scalp is not the main perpetrator causing the disappearance of the non-linearity in EEG signals, since

TABLE I  
CORRELATION VALUES FOR TWO MODELS

Model	Thumb	INDEX	Middle	RING	Pinky
LMR	0.4016	0.6722	0.0876	0.4470	0.2344
ANN	0.4015	0.6935	0.1010	0.4601	0.2426

this is also observed in ECoG signals. This suggests that the spatio-temporal summation of multiple neural signals is itself linearly correlated with movement, and is not an artifact introduced by the scalp or cranium.

#### ACKNOWLEDGMENT

This project was supported by NIH Grants R01-052345 and R01-050520 to FV-C, and University of Southern California Graduate School's Provost Fellowship to AM. We also want to acknowledge Amir Ahmadi for his helpful comments on this manuscript.

#### REFERENCES

- [1] A. Geramipour, M. Khazaei, A. Marjaninejad, and M. Khazaei, "Design of FPGA-based digital PID controller using Xilinx SysGen for regulating blood glucose level of type-I diabetic patients," *Int J Mechatron Electr Comput Technol*, vol. 3, no. 7, pp. 56–69, 2013.
- [2] A. Marjaninejad and S. Daneshvar, "A low-cost real-time wheelchair navigation system using electrooculography," in *Electrical Engineering (ICEE), 2014 22nd Iranian Conference on*, 2014, pp. 1961–1965.
- [3] R. Fukuma *et al.*, "Real-time control of a neuroprosthetic hand by magnetoencephalographic signals from paralysed patients," *Sci. Rep.*, vol. 6, 2016.
- [4] A. Marjaninejad, F. Almasganj, and A. J. Sheikhzadeh, "Online signal to noise ratio improvement of ECG signal based on EEMD of synchronized ECG beats," in *Biomedical Engineering (ICBME), 2014 21th Iranian Conference on*, 2014, pp. 113–118.
- [5] H. C. Sox, *Medical decision making*. ACP Press, 1988.
- [6] L. F. Nicolas-Alonso and J. Gomez-Gil, "Brain computer interfaces, a review," *Sensors*, vol. 12, no. 2, pp. 1211–1279, 2012.
- [7] M. Shanechi, R. Hu, M. Powers, and G. Wornell, "Neural population partitioning and a concurrent brain-machine interface for sequential motor function," *Nature*, 2012.
- [8] F. J. Valero-Cuevas, "An integrative approach to the biomechanical function and neuromuscular control of the fingers," *J. Biomech.*, vol. 38, no. 4, pp. 673–684, 2005.
- [9] J. M. Inouye, J. J. Kutch, and F. J. Valero-Cuevas, "Optimizing the topology of tendon-driven fingers: Rationale, predictions and implementation," in *The Human Hand as an Inspiration for Robot Hand Development*, Springer, 2014, pp. 247–266.
- [10] C. Klaes *et al.*, "Hand Shape Representations in the Human Posterior Parietal Cortex," *J. Neurosci.*, vol. 35, no. 46, pp. 15466–15476, 2015.
- [11] F. Lotte, M. Congedo, A. Lécuyer, F. Lamarche, and B. Arnaldi, "A review of classification algorithms for EEG-based brain-computer interfaces," *J. Neural Eng.*, vol. 4, no. 2, p. R1, 2007.
- [12] T. Aflalo *et al.*, "Decoding motor imagery from the posterior parietal cortex of a tetraplegic human," *Science (80-. )*, vol. 348, no. 6237, pp. 906–910, 2015.
- [13] N. Liang and L. Bougrain, "Decoding finger flexion from band-specific ECoG signals in humans," *Front. Neurosci.*, 2012.
- [14] Y. J. Kim *et al.*, "A study on a robot arm driven by three-dimensional trajectories predicted from non-invasive neural signals," *Biomed. Eng. Online*, vol. 14, no. 1, p. 81, 2015.
- [15] D. Garrett, D. A. Peterson, C. W. Anderson, and M. H. Thaut, "Comparison of linear, nonlinear, and feature selection methods for EEG signal classification," *IEEE Trans. neural Syst. Rehabil. Eng.*, vol. 11, no. 2, pp. 141–144, 2003.
- [16] J. Sanchez, A. Gunduz, and P. Carney, "Extraction and localization of mesoscopic motor control signals for human ECoG neuroprosthetics," *J. Neurosci.*, 2008.
- [17] G. Schalk *et al.*, "Decoding two-dimensional movement trajectories using electrocorticographic signals in humans," *J. Neural Eng.*, vol. 4, no. 3, p. 264, 2007.